Electronic and optical properties of InAs(110)

X. López-Lozano[a], C. Noguez[b,*], and L. Meza-Montes[a]

[a]*Instituto de Física, Universidad Autónoma de Puebla,*
Apartado Postal J-48, Puebla 72570, México
[b]*Instituto de Física, Universidad Nacional Autónoma de México,*
Apartado Postal 20-364, Distrito Federal 01000, México

The electronic and optical properties of the cleavage InAs(110) surface are studied using a semi-empirical tight-binding method which employs an extended, atomic-like, basis set. The surface electronic states are discussed in terms of their electronic character, and compared with other theoretical approaches, and experimental observations. The surface electronic band structure and the Reflectance Anisotropy Spectrum (RAS) are calculated and discussed in terms of the surface electronic states and the atomic structure of the surface.

Keywords: Surface reconstruction; surface states; reflectance anisotropy; differential reflectance; semiconductor surface; indium arsenide; III-V surface.

Las propiedades ópticas y electrónicas de la superficie InAs(110) se estudiaron usando el modelo de enlace fuerte y una base extendida tipo atómica. Se discute el carácter de los estados electrónicos asociados a la superficie y se comparan los resultados con otras aproximaciones teóricas y medidas experimentales. Se calculan las propiedades ópticas de la superficie y se analizan en términos del espectro de Reflectancia Anisoptrópica y de los estados electrónicos de superficie y de la estructura atómica.

Descriptores: Reconstruccón superficial; estados de superficie; reflectancia anisotrópica; reflectancia diferencial; superficie semiconductora; arsenuro de indio; superficie III-V.

PACS: 78.68.+m; 73.20.At; 78.55.Cr; 78.66.Fd

1. Introduction

The (110) surface is the natural cleavage of zincblende crystals, and it is a non-polar surface which contains equal number of cations and anions in its unit cell, showing a partly ionic bonding. The mechanism of reconstruction and the electronic properties of the (110) surface of III-V semiconductors seems to be understood in general terms, [1–7] but this is not in detail. A lot of theoretical work has been done to determine the electronic properties of Gallium compounds and their surfaces. On the other hand, only a few attempts have been made to characterize the InAs surfaces, where there is no agreement between theoretical results and experimental measurements reported in the literature. Therefore, more theoretical and experimental studies are necessary.

Most of the theoretical studies [8–12] about InAs(110) do not provide a way to directly compare them with experiments [13–23]. Furthermore, the available experimental measurements are not enough to completely elucidate the atomic structure and electronic properties of InAs(110). For example, Andersson and collaborators [13, 14] found the energies of occupied-surface states at high-symmetry points using photoemission techniques. Independently, Swantson *et al.* [15] also measured the energies of occupied-surface states at high-symmetry points, and they found differences of up to 0.5 eV with those reported by Andersson and collaborators [14]. In general, the interpretation of photoemission spectra has been difficult to do because of the small bulk-band gap of InAs.

Theoretically, the electronic structure and atomic positions of InAs(110) were calculated using a total-energy minimization scheme [9] based on a semi-empirical, tight-binding (TB) approach. Almost a decade latter, an *ab initio* quantum-molecular dynamics [8] was performed. The reported atomic structure and electronic surface states differ between TB and *ab initio* calculations, and also differ with the available experimental measurements. This is because the semi-empirical calculations were performed using an atomic reconstruction that was not fully relaxed. The *ab initio* calculation was performed using DFT-LDA with a plane-wave basis set whose accuracy was compromised with the choice of several approximations such as energy cut-off, obsolete pseudopotentials, etc. Therefore, the *ab initio* calculation [8] presented systematic errors in determining the surface electronic energy levels. Although *ab initio* methods are better than empirical ones, it is well-known that such methods are far from easy to implement. For example, it is known that for small band gap semiconductor crystals, such as Ge, InAs, etc., *ab initio* methods predict a negative gap or metallic behavior. It is also known that *ab-initio* methods need to use a large cut-off energy to achieve convergence in surface electronic states, and incorporate many-body electron interactions to obtain the correct energy from them. Therefore, semi-empirical methods expected to be more suitable than ab initio calculations for the InAs(110) surface. We believe that it is for this reason that only one *ab initio* calculation is found in the literature.

The optical properties of InAs(110) have also been investigated, both, theoretically and experimentally. Shkrebtii and collaborators [12] calculated and measured the Reflectance

Anisotropy Spectrum (RAS) of InAs(110). Although the authors claimed to elucidate the optical properties of this surface, the calculated RAS is far from resembling their measurements. In summary, with the available theoretical and experimental evidence, it is no possible to clearly elucidate the main electronic and optical properties of InAs(110). In this work, we study the electronic structure and optical properties of InAs(110), employing a semi-empirical TB formalism [24, 25], and using the atomic coordinates obtained from *ab initio* quantum-molecular dynamics [8]. The use of the fully relaxed atomic coordinates guarantees that the calculated electronic properties will include all the subtle effects of surface-induced strain and appropriate geometry. The TB approach allows us to analyze in detail the electronic structure and optical properties, and compare our calculations with available experimental data.

2. Theoretical method

The III-V(110) semiconductor surfaces relax in such a way that the surface cation atom moves inwards the surface into an approximately planar configuration, with a threefold coordination with its first-neighbor anion atoms. The topmost anion atom moves outward to the surface, showing a pyramidal configuration with its three first-neighbor cation atoms [2, 3]. The geometric parameters that describe the relaxation of the surface atoms of III-V(110) semiconductor surfaces, scale linearly with the bulk lattice constant [3]. In particular, Alves *et al.* found [8] that for the InAs(110) surface the *pyramidal* angle at the anion, labeled α, is $\sim 90°$, the *in-plane* angle β has values close to the tetrahedral bond angle $\sim 109.47°$, and the *planar* angle at the cation, labeled by γ, is $\sim 120°$. For the ideal surface the values for α, β and γ correspond to those angles of tetrahedral bonds, $109.47°$.

The relaxed InAs(110) surface is shown in Fig. 1. In Fig. 1(a) we show the top view of a surface unit cell that contains one In atom (cation), and one As atom (anion) per atomic layer. The open circles correspond to As atoms, while black circles show In atoms. The parameter a_0 is the bulk lattice constant and $d_0 = a_0/2\sqrt{2}$. The larger side of the unit cell is along the [001] crystallographic direction, while the shorter side is along the [1$\bar{1}$0]. In Fig. 1(b), we show a side view with only the three outermost atomic layers of the surface. Here, we define the structural parameters associated with the surface relaxation whose values are given in Table I. In Fig. 1(c), we show the corresponding Two-Dimensional Irreducible Brillouin Zone (2DIBZ).

In our calculations, the non-polar InAs (110) surface was modeled using a slab of 50 atoms, yielding a free reconstructed surface on each face of the slab. The thickness of the slab is large enough to decouple the surface states at the top and bottom surfaces of the slab. Periodic boundary conditions were employed parallel to the surface of the slab to effectively model an infinite, two-dimensional crystal system. The atomic coordinates were taken from Ref. 8, and are given

TABLE I. Structural parameters as defined in Fig. 1. Parameters obtained from DFT calculations using an energy cutoff of 8 Ry (*), and 18 Ry (**), both from Ref. 8, and parameters from Low-Energy Electron Diffraction (LEED) measurements from Ref. 22.

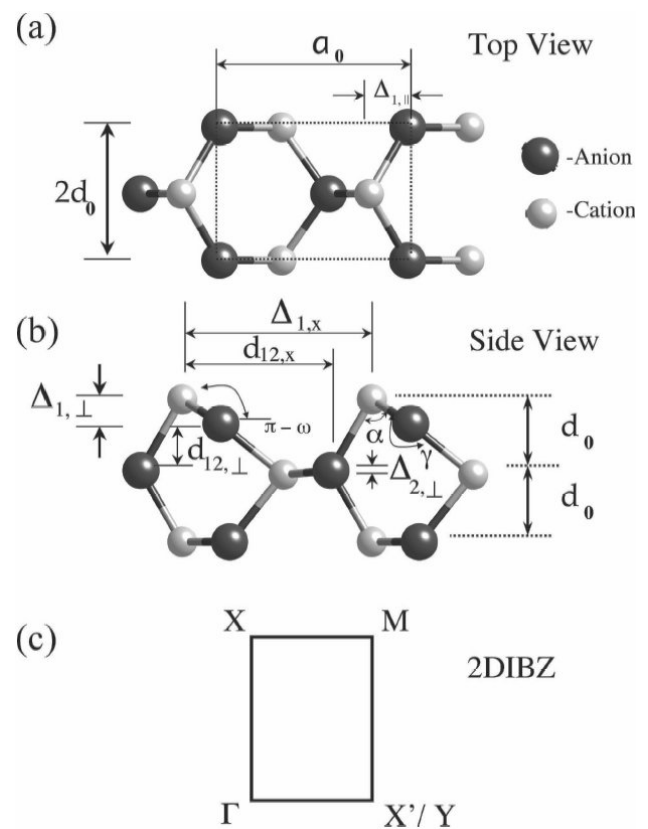|	a_0 (Å)	$\Delta_{1,\perp}$ (Å)	$\Delta_{1,x}$ (Å)	$\Delta_{2,\perp}$ (Å)	$d_{12,\perp}$ (Å)
Ideal	6.04	0.0	$3/4a_0$	0.0	d_0
DFT*	5.844	0.70	4.656	0.122	1.463
DFT**	5.861	0.75	4.663	0.128	1.445
LEED	6.036	0.78	4.985	0.140	1.497
	$d_{12,x}$(Å)	ω (deg)	(%)c_1a_1	(%) c_2a_1	(%)c_1a_2
Ideal	$a_0/2$	0.0	0.0	0.0	0.0
DFT*	3.361	30.7	-1.80	-0.22	-2.00
DFT**	3.395	32.0	-1.18	-0.18	-1.82
LEED	3.597	36.5	-4.22	$+2.03$	—

FIGURE 1. Model of the atomic geometry of InAs(110). (a) Top view of a surface unit cell. (b) Side view of the first three atomic layers of the surface. (c) Two-Dimensional Irreducible Brillouin Zone.

in Table I. We have performed calculations with all the structural parameters in Table I, however, those corresponding to the Density Functional Theory [8] (DFT) with an energy cutoff of 18 Ry are the ones that best resemble some experimental data [13–23]. We calculate the electronic level structure of the slab using a well-known parameterized TB approach with a sp^{3}s* orbital-like basis, within a first-neighbor interaction

approach [25]. This wave function basis provides a good description of the valence and conduction bands of cubic semiconductors, except along the X – W direction in the Brillouin zone where the conduction bands are underestimated. TB calculations for bulk III-V semiconductors have shown that d orbitals are of crucial importance for the lowest two conduction bands at X [26]. The sp^3s^* TB approximation has been applied to calculate the electronic and optical properties of a variety of semiconductor surfaces, including other III-V compounds [6]. The TB parameters are taken to be the same as those of Vogl [25] for the bulk but they are scaled by a factor of $(D/d)^2$, where d is the bond length of any two first-neighbor atoms, and $D = \sqrt{3}a_0/4$. [27] These changes to the original bulk parameters provide an excellent description of the electronic structure as compared to experimental measurements. To distinguish between surface and bulk electronic states, we have projected the total wave function onto the atomic orbitals belonging to the outermost atoms of the slab.

Once the electronic-level structure of the slab has been obtained, we calculate the average slab polarizability in terms of the transition probabilities between eigenstates induced by an external radiation field. We take an average over 4096 points distributed homogeneously in the irreducible two-dimensional Brillouin zone (2DBZ). The real part of the average polarizability is calculated using the Kramers-Kronig relations. Finally, the RAS is calculated as the difference in Differential Reflectance between two orthogonal directions in the surface plane, such as

$$\text{RAS} = \left(\frac{\Delta R}{R_0}\right)_{[1\bar{1}0]} - \left(\frac{\Delta R}{R_0}\right)_{[001]}, \qquad (1)$$

where R_0 is the bulk reflectivity calculated with the well-known Fresnel formula, and $\Delta R = R - R_0$ is the difference between R_0 and the actual reflection coefficient. The details are fully explained in Ref. 24.

The atomic structure of the surface region is intimately related to its electronic structure. Experimentally, the electronic structure can be determined by means of electron spectroscopies such as photoemission (PE), inverse photoemission (IPE), and Scanning Tunneling Spectroscopy (STS). These techniques are sensitive to the surface's features and electronic properties due to relaxation, reconstruction or adsorption events. In Section III we present and discuss the surface electronic band structure and the local density of electronic states of InAs(110), and in Section IV, we discuss the results of the optical properties.

3.   Surface Electronic Structure

3.1.   Results

We show the surface electronic band structure along high-symmetry points of the 2DIBZ of the relaxed InAs(110) surface in Fig. 2. The projected bulk electronic states are indicated in tiny black dots, while the surface electronic states

are indicated in large black dots. We denote the surface electronic states using the labels A_i and C_i associated with the surface anions and cations, respectively, as introduced by Chelikowsky and Cohen [28]. The calculated average of the Fermi energy level for the surface, E_F^s, is at 1.1 eV above the Valence-Band-Maximum (VBM). For InAs(110), there is no agreement between the measurements of E_F^s; however, all of these experiments show that the value of E_F^s increases with respect to the bulk Fermi level that is found at 0.55 eV. For bulk InAs, we found that E_F^b is about 0.6 eV, in good agreement with experimental observations [14].

Below the VBM, we found four well-defined occupied surface electronic states denoted by A_5, A_3, A_2 and C_2. The A_5 surface states correspond to the dangling bonds of the As atoms located in the first atomic layer. The A_5 states form a band from the high-symmetry point X to the point X′, going through the high-symmetry point M in the 2DIBZ. This band has a minimum at X with an energy of -1.20 eV and disperses upwards towards the Γ point. From X, the band also disperses upwards towards the M point, where the A_5 surface states have an energy of about -0.8 eV. From M to X, this band disperses into the projected bulk band. The A_5 band shows a small dispersion around M, giving rise to a large contribution to the Local Density of States (LDOS) in the first layer at an energy of about -1 eV, as shown in Fig. 3.

The A_3 surface electronic states are at a lower energy than A_5. The A_3 states are due to the backbonds between the anions situated in the first atomic layer and the cations in the second layer. The A_3 band has a minimum in the X high-symmetry point, with an energy of -2.8 eV from the VBM. The band reaches its maximum at X′ with an energy of -1.6 eV from the VBM. The band shows a dispersion of 1.2 eV; however, around X and M the band is almost flat, contributing to a large density of states in the first and the second layers at energies of about -2.8 eV and -2.5 eV, respectively.
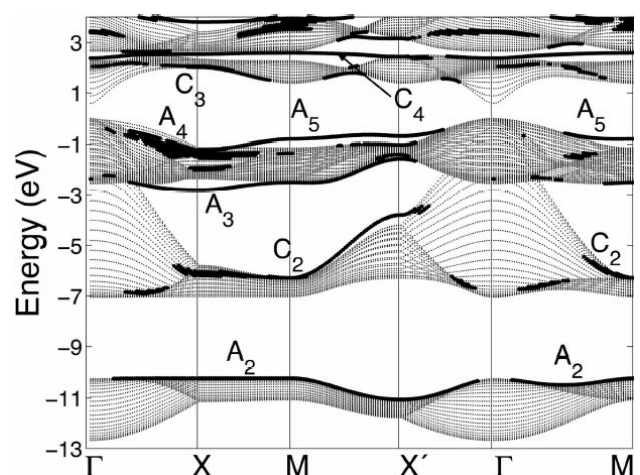

FIGURE 2.   Electronic band structure of the reconstructed InAs(110) surface. Tiny dots represent the projected bulk states, while black dots represent surface electronic states.
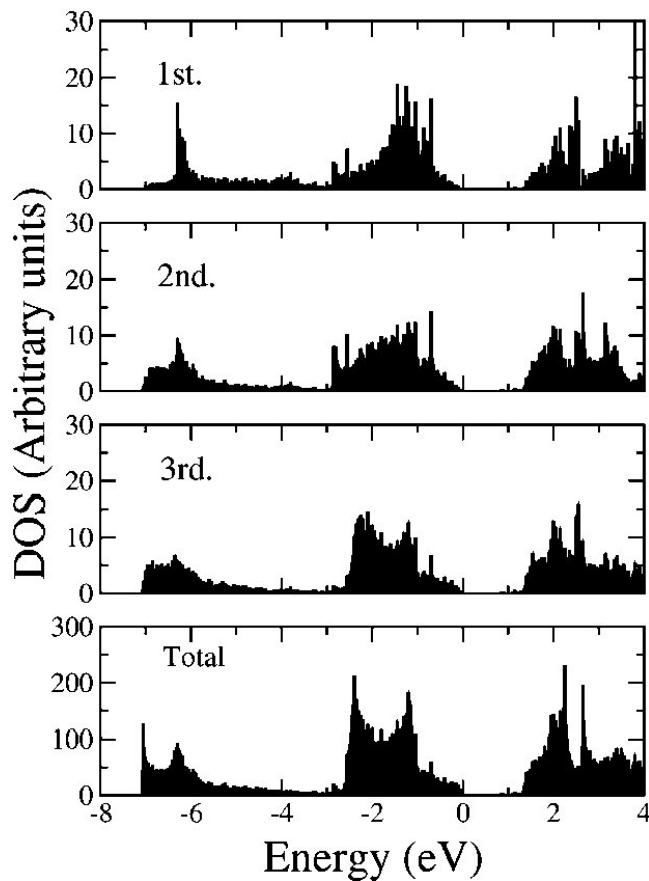
FIGURE 3. Total and projected local density of states in the first, second and third atomic layers of reconstructed InAs(110).

This can be observed on the LDOS in Fig. 3, where two peaks are found at these energies in the panels showing the LDOS in the first and second layers.

We found surface states with an energy of about -6.0 eV at the high-symmetry point X that form a band denoted by C_2. This band shows a large dispersion of about 2.5 eV, where the minimum of the band is at M with an energy of -6.3 eV, and its maximum is around X$'$ with an energy of -3.8 eV. These surface states are located at the cation (In) atoms and are due to the bonding between the In and As atoms at the top layer. From X to M, the band shows a small dispersion which is reflected in the LDOS, where a large contribution is found at about -6.2 eV in the panel showing the projected LDOS in the first layer in Fig. 3. From M to X$'$, the C_2 band disperses upwards of about 2.5 eV, giving rise to a small contribution to the LDOS, as shown in Fig. 3.

At lower energies we found another occupied surface electronic band, denoted by A_2, which extends completely almost along the high-symmetry points in the 2DIBZ. These surface states are located in the anion (As) atoms, and have an s character due to the backbonds between the atoms at the first and second layers, and some contribution is also found from the backbonds between the atoms in the second and third layers. From Γ to M along X, the band does not show dispersion and is at -10.2 eV. From M to Γ along X$'$, the

band has a dispersion of about 1 eV, showing a minimum around X$'$.

We have also found several states situated at X between Γ and M with an energy from -2 eV to -1 eV. These states are inside the projected bulk band, and are therefore resonance-like states. These resonance states, denoted by A_4, disperse upwards from X towards both Γ and M. Most of the A_4 states have a p-character, and are localized at the anion in the first atomic layer. The A_4 states with lower energy, between -1.9 eV and -2.0 eV, show also an s character and are localized at the third layer.

Above the VBM, we found two unoccupied surface states bands, namely, C_3 and C_4. The C_3 surface states are situated at the cations in the first and third atomic layers. They show a strong p character due to the dangling bonds at the cations. At X, we found that C_3 has a maximum with an energy of about 2 eV, and has its minimum value between M and X$'$ with an energy of about 1.4 eV. Finally, at 2.7 eV from VBM we found empty surface states that form a band all along the high symmetry points in the 2DIBZ. This band is denoted by C_4, and shows a very small dispersion along the 2DIBZ.

3.2. Discussion

In this section we discuss our results, and compare them with theoretical calculations [8–12] and experimental measurements [13–23]. The electronic properties of InAs(110) have been investigated previously using experimental techniques such as photoemission (PE) [13–18] and inverse photoemission (IPE) [18–21] spectroscopies. We found no agreement between experimental measurements because they present difficulties in identifying the position of the VBM or E_F, and the samples employed are quite different. Furthermore, photoemission measurements are difficult to interpret, since emissions from surface states are usually hidden by emissions from bulk states in InAs surfaces, due to the small bulk-band gap.

On the other hand, theoretical calculations have been performed using *ab initio* [8] and semi-empirical TB [9–12] methods. We summarize our results and some of the experimental and theoretical data in Table II, where we show the energy values at high-symmetry points in 2DIBZ of the surface electronic states denoted by A_5, A_3, A_4 and C_2. The first column shows our results, the next three columns show experimental measurements obtained by PE [13–15], and the last two columns show theoretical results [8,9]. The values in Table II are those reported in the corresponding reference, or they have been estimated from the figures in each reference, and so errors of about 0.1 eV in the estimated values are expected.

Alves *et al.* [8] performed an *ab initio* calculation based on the Density Functional Theory (DFT) within the Local Density Approximation (LDA), where many-body effects were not taken into account. They considered slabs of only eight atomic layers (16 atoms), and the plane-wave basis set employed was expanded up to an energy cutoff of 8 and

TABLE II. Experimental and theoretical values of the surface states at high-symmetry points of the 2DIBZ. The energy values are in eV, where the zero energy corresponds to the VBM. (†) Estimated value from Fig. 7(a) in Ref. 8. (*) Estimated values from Fig. 9(b) in Ref. 9.

State	This work	PE [13]	PE [14]	PE [15]	DFT [8]	TB* [9]
$A_5(\Gamma)$		−0.30	−0.45	−0.53		−0.3
$A_5(X)$	−1.21	−1.00	−1.15	−0.83	−0.85	−0.9
$A_5(X'/Y)$	−0.70	−0.85	−1.00	−0.73		−0.7
$A_5(M)$	−0.81		−1.10	−0.70		−0.8
$A_3(\Gamma)$			−2.60			−2.1
$A_3(X)$	−2.81	−3.1	−3.25	−2.72	−3.21	−3.1
$A_3(X'/Y)$	−1.57		−1.50			−1.4
$A_3(M)$	−2.51		−3.40			−2.7
$C_2(\Gamma)$		−3.35	−3.50			−3.2
$C_2(X)$	−6.04			−4.90		−5.8
$C_2(X'/Y)$	−3.8	−3.7	−3.85	−3.35	−3.4†	−3.6
$C_2(M)$	−6.28		−6.10		−5.46	−6.1
$A_4(\Gamma)$			−0.45			−0.6
$A_4(X)$	−1.53	−1.6	−1.75			−1.2
$A_4(X'/Y)$	−1.36	−1.05	−1.20			−0.9
$A_4(M)$	−1.03		−1.10			−1.0

18 Ry. They reported results for the equilibrium atomic structure and the electronic band structure. It is known that the equilibrium atomic geometries can be found with good accuracy, but an underestimate and/or overestimate of electronic states is always present in DFT-LDA calculations due to the approximations employed; for example, DFT usually neglects many-body effects [29]. Furthermore, plane-wave basis expansions always present convergence problems in finding localized states. Therefore, the comparison of the surface states from *ab initio* calculations [8] with semi-empirical results and PE measurements always presents deviations up to ±1 eV. We also compare our results with semi-empirical TB calculations done by Mailhiot *et al.* [9]. These TB calculations employed a theoretical method similar to the one used here but with different atomic positions, that were not fully relaxed.

Both theoretical calculations [8, 9] found an empty surface state C_3, and this was identified with dangling bond states at the cations. While the DFT calculation [8] found that C_3 has a minimum at X, we obtained a maximum at the same symmetry point in agreement with other semi-empirical calculations [9–12]. DFT calculations reported an upwards dispersion from X of about 1.4 eV, while we found a downwards dispersion from X of about 0.6 eV. This discrepancy between DFT and semiempirical calculations is to be expected, since DFT uses a plane-wave basis set that can not reproduce conduction states, while semiempirical calculations with an extended basis set can. The C_3 surface states have been mea-

sured by using inverse photoemission [18–21], but only at the X high-symmetry point. Experimental measurements assigned an energy of between 1.7 eV and 1.9 eV at X, and evidence of an upwards dispersion from this point have been observed [18], in agreement with our calculations. However, a more detailed experimental analysis is necessary in order to reach further conclusions about empty states.

The occupied surface states denoted by A_5, A_3, and C_2, were also calculated in Refs. 8 and 9. Both calculations identified the A_5 surface states with the dangling bond states in the anion atoms, in agreement with our results. The A_5 surface state found using a first-principles method [8] is shifted 0.3 eV on the average, above both the experimental value [14] and our calculation. Experimentally [14], the A_5 surface state has a dispersion of about 0.15 eV from X to X′ through M, while we calculate a dispersion of 0.5 eV, similar to the one obtained using DFT [8]. The surface states denoted by A_4 have been also observed experimentally [13, 14], and calculated by Mailhiot *et al.* [9]. As in the case of the A_5 states, we are unable to identify A_4 states at the Γ point. PE measurements showed that these states have a dispersion of about 0.55 eV from X to to X′ through M, which is in agreement with our calculated value of 0.5 eV, while Mailhiot *et al.* [9] found a smaller dispersion of 0.2 eV, and this value was not calculated using DFT [8]. Previous semiempirical results [9] also found the occupied states labeled by A_4; however, these surface states were not well identified since in their calculations the A_4 states show a dispersion very similar to the A_5 states. In general, the A_4 are resonant states and they are difficult to calculate, especially if a plane-wave basis is used as in the DFT calculations discussed here [8]. Below A_4, other resonant states have been observed denoted by A_3, using PE [14]. The data reported for A_3 are quite different from our calculations and previous TB calculations [9], perhaps because the identification of these states is not clear experimentally [13, 14]. On the other hand, the C_2 states can be experimentally identified since they are in a gap, except at the X point where they disperse into the projected bulk states.
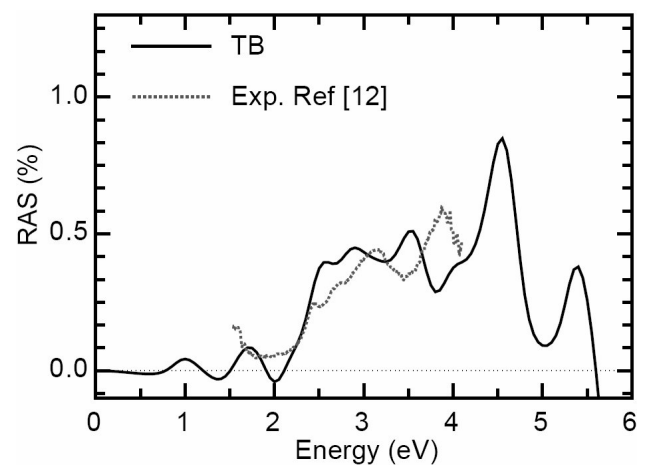

FIGURE 4. Reflectance Anisotropy Spectrum calculated by us (dotted line), and measured (solid line) in Ref. 12.
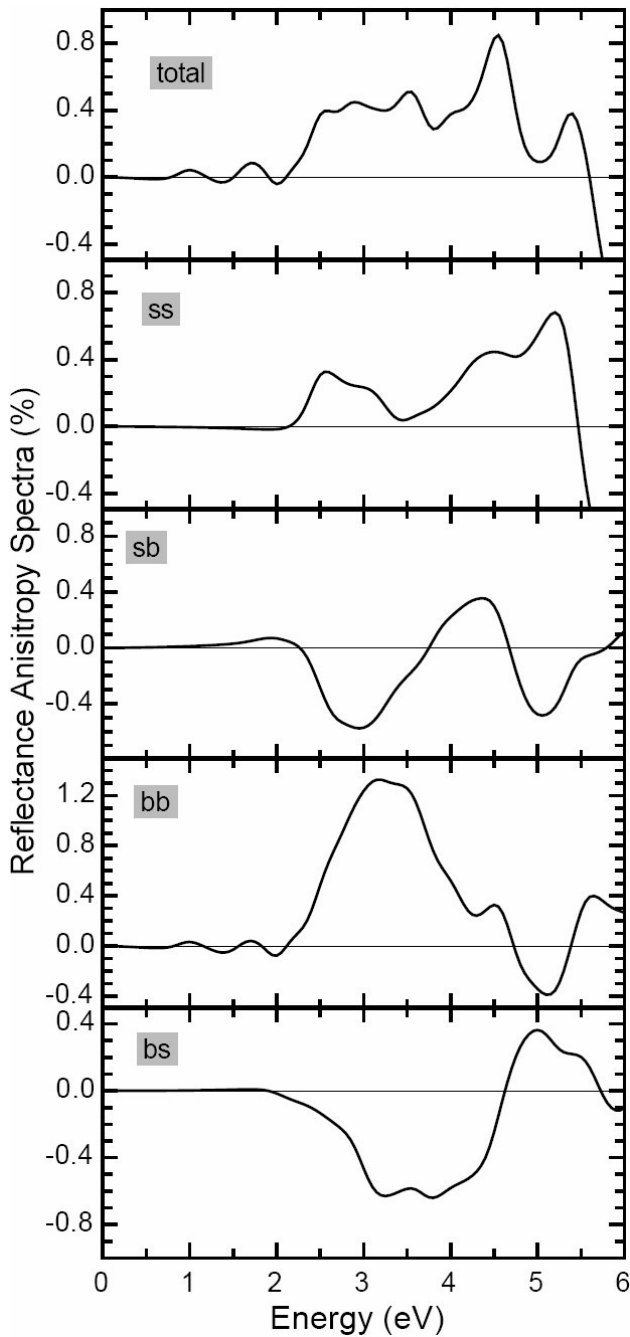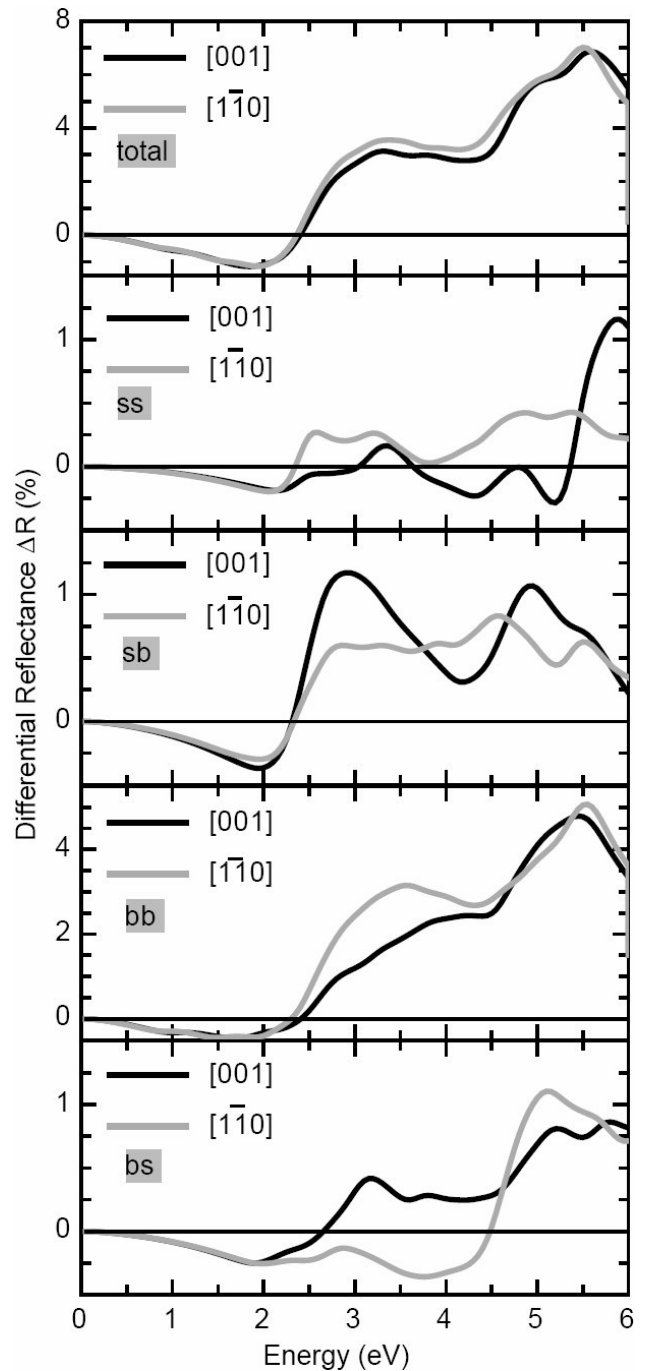
FIGURE 5. Total calculated RAS and its components.

FIGURE 6. ΔR along the main directions on the surface plane.

4. Optical Properties: Results and Discussion

We calculate the Reflectance Anisotropy Spectrum (RAS) according to Eq. (1) for InAs(110) as a function of the energy of the incident light. RAS has contributions of electronic transitions from occupied to empty states which are labeled as surface to surface (*ss*), surface to bulk (*sb*), bulk to bulk (*bb*), and bulk to surface (*bs*) electron transitions. The bulk-band gap is less than 0.5 eV, so that *bb* transitions due to modified bulk states are important over the entire the spectrum. In Fig. 4, we show the calculated RAS, and we compared our

results with measurements from Ref. 12. The experimental RAS was measured from 1.5 to 4.5 eV, and it is always positive. In Fig. 5, we show the calculated RAS indicated as by total and its decomposition due to the different contributions *ss*, *sb*, *bb*, and *bs*. In general, our calculated RAS resembles the main features of the measured RAS more closely than a previous calculated spectrum [12].

In Ref. 12, the peak around 2.5 eV is assigned to *ss* transitions, while we found that this peak has contributions from all kinds of electron transitions involving surface states as well as modified bulk states. The calculated structure at 2.75 eV

is also observed experimentally [12] at 3.1 eV. Again, we observed that this peak is related to all kind of electron transitions, while Shkrebtii *et al.* [12] associated it with modifications of bulk states at E_1, the critical point. They also found [12] that the main features of RAS at higher energy are due to *bb* transitions only. However, we found that *bb* transitions are important around 3.2 eV, and not at higher energies. Experimentally, a peak was found at 3.8 eV, while we found it at 3.5 eV. We believe that these discrepancies at the energy location are due to our tight-binding approximation which underestimates the electron energies around the X high-symmetry point. However, we have found a good agreement between our calculations and experimental results. Below, we explain in detail the main features of the calculated RAS.

We found that below 2 eV the spectrum is dominated by transitions between modified bulk states (*bb*), and they have a small intensity. However, the electron transitions among modified bulk states become important at around 3 eV. Also, some *sb* transitions are present at around 1.5 eV, which slightly modify the lineshape of the spectrum. From 2 eV, the contributions from all kinds of electron transitions involving surface states become important. In Fig. 6, we show the differential reflectance ΔR as defined in Eq. 1 along the main crystallographic directions on the surface plane. We observe that *ss* transitions have a smaller intensity than the other transitions; however, *ss* transitions are very anisotropic and so they have an important contribution to the spectrum from 2 to 6 eV, as seen in Fig. 5. The *ss* transitions occur mainly at about 2.5, 3.4 and from 4 to 6 eV. The first two peaks at lower energies are transitions from A_5, and A_4 surface states to C_3 surface states, due to dangling bonds located at the surface As and In atoms, respectively. The broad structure from 4 to 6 eV is due to *ss* transitions from A_3 occupied surface states to C_3 empty surface states. The *sb* electron transitions are also anisotropic and contribute to RAS from 2 to 6 eV. Along the [001] direction, the spectrum is more intense, and has two peaks, at 2.9 and 4.9 eV. The first peak, at 2.9 eV is due to transitions from A_5, and A_4 surface states to empty bulk states around 2.2 eV, where the density of states is large (see Fig. 3). The second peak at 4.9 eV is due to electron transitions from A_3 occupied surface states to the same empty bulk states around 2.2 eV. We also found that *bs* transitions play an important role in RAS. These transitions have a small intensity, but they are also very anisotropic. The main contribution of *bs* to RAS is from 3 to 6 eV, where the occupied bulk states are those from -1 eV to -2.8 eV, as shown in the total DOS. The electron transitions occur from these states to empty surface states C_3 located around 2.2 eV.

5. Summary

We performed a tight-binding calculation using a fully relaxed atomic geometry to study the electronic structure and optical properties of the clean InAs(110) surface. A very detailed analysis was done, and a good agreement between our calculations and experimental data was found. We found that fully relaxed atomic positions from *ab initio* methods, in combination with our semi-empirical, tight-binding calculation, better resemble photoemission and Reflectance Anisotropy Spectrum measurements of the cleavage InAs(110) samples. We explain the main features of the optical spectrum and relate these to surface atomic relaxation and electronic structure. Although the agreement between our results and other theoretical and experimental data is good, we conclude that more experimental studies are necessary to clearly elucidate the atomic relaxation and electronic properties of InAs(110).

∗. Author to whom correspondence should be addressed. E-mail: cecilia@fisica.unam.mx

1. *Group III Nitride Semiconductors Compounds: Physics and Applications*, edited by B. Gil (Oxford Science Publications, Great Britain, 1998).

2. See for example, F. Bechstedt and R. Enderlein, *Semiconductor Surfaces and Interfaces* (Akademie-Verlag, Berlin, 1988); A. Zangwill, *Physics at Surfaces* (Cambridge University Press, New York, 1992); H. Lüth, *Surfaces and Interfaces of Solids* (Springer Verlag, Berlin, 1993).

3. T.J. Godin, J.P. LaFemina, and C.B. Duke, *J. Vac. Sci. Technol. A* **10** (1992) 2059.

4. O. Pulci, G. Onida, R. Del Sole, and A.J. Shkrebtii, *Phys. Rev. B* **58** (1998) 1922.

5. O. Pulci, B. Adolph, U. Grossner, and F. Bechstedt, *Phys. Rev. B* **58** (1998) 4721.

6. C. Noguez, *Phys. Rev. B* **58** (1998) 12641; *ibid* **62** (2000) 2681.

7. G. Cappellini, G. Satta, M. Palummo, and G. Onida, *Phys. Rev. B* **66** (2002) 115412.

8. J.L. Alves, J. Hebenstreit and M. Sheffler, *Phys. Rev. B* **44** (1991) 6188.

9. C. Mailhiot, C.B. Duke, and D.J. Chadi, *Phys. Rev. B* **31**, 2213 (1985).

10. R. P. Beres, R. E. Allen and J. D. Dow, Phys. Rev. B **26** (1982) 5207.

11. B. Engels *et al.*, *Phys. Rev. B* **58** (1998) 7799.

12. A.I. Shkrebtii *et al.*, *Appl. Surf. Sci.* **104/105**, 176 (1996).

13. C.B.M. Andersson, J.N. Andersen, P.E.S. Persson, and U.O. Karlsson, *Phys. Rev. B* **47** (1992) 2427.

14. C.B.M. Andersson, J.N. Andersen, P.E.S. Persson and U.O. Karlsson, *Surf. Sci.* **398** (1998) 395.

15. D.M. Swantson *et al.*, *Surf. Sci.* **312** (1994) 361.

16. D.M. Swantson *et al.*, *Can. J. Phys* **70** (1992) 1099.

17. H. W. Richter *et al.*, *J. Vac. Sci. Technol. B* **4** (1986) 900.

18. H. Carstensen, R. Claessen, R. Manzke, and M. Skibowski, *Phys. Rev. B* **41** (1990) 9880.

19. W. Drube, D. Straub, and F.J. Himpsel, *Phys. Rev. B***35** (1987) 5563.

20. W. Gudat and D.E. Eastman, *J. Vac Sci. Technol.* **13** (1976) 831.

21. J. van Laar, A. Huiser, and T.L. van Rooy, *J. Vac Sci. Technol.* **14** (1977) 894.

22. C. Mailhiot, C.B. Duke, and D.J. Chadi, *Surf. Sci.* **149** (1985) 366.

23. C. B. Duke, A. Paton, A. Kahn, and C.R. Bonapace, *Phys. Rev. B* **27** (1983) 6189.

24. C. Noguez and S.E. Ulloa, *Phys. Rev. B* **53** (1996) 13138; and references therein.

25. P. Vogl, H.P. Hjalmarson, and J.D. Dow, *J. Phys. Chem. Solids* **44** (1983) 365.

26. J.-M. Jancu, R. Scholz, F. Beltram, and F. Bassani, *Phys. Rev. B* **57** (1998) 6493.

27. *"Electronic Structure and the Properties of Solid"*, Walter A. Harrison (Dover Publications, Inc., New York, 1980).

28. J.R. Chelikowsky and M.L. Cohen, *Solid State Commun.* **29** (1979) 267.

29. M.S. Hybertsen and S.G. Louie, *Phys. Rev. B* **34** (1986) 5390; *ibid* **38** (1988) 4033; F. Bechstedt and R. Del Sole, *ibid* **38** (1988) 7710; R. Godby, M. Schlüter, and L.J. Sham, *ibid* **37** (1988) 10159.